Electronic Supplementary information for

Surface-enhanced Raman scattering imaging of cancer cells and tissues via sialic acid-imprinted nanotags

Danyang Yin,[a] Shuangshou Wang,[a] Yunjie He,[b] Jia Liu,[a] Min Zhou,[c] Jian Ouyang,[c] Baorui Liu,[b] Hong-Yuan Chen,[a] and Zhen Liu*,[a]

[a] State Key Laboratory of Analytical Chemistry for Life Science and Collaborative Innovation Center of Chemistry for Life Sciences, School of Chemistry and Chemical Engineering, Nanjing University, Nanjing 210093, PR China

[b] The Comprehensive Cancer Center of Drum Tower Hospital, Medical School of Nanjing University & Clinical Cancer Institute of Nanjing University, Zhongshan Road 321, Nanjing 21008, PR China

[c] Department of Hematology, The Affiliated Drum Tower Hospital of Nanjing University Medical School, Nanjing 210008, PR China

* To whom correspondence should be addressed. E-mail: zhenliu@nju.edu.cn

Experimental

Materials and apparatus. 3-Aminopropyltriethoxysilane (APTES, 98%), dimethyl sulfoxide (DMSO, 99%), tetraethylorthosilicate (TEOS, 99%), *p*-aminothiophenol (PATP) and horseradish peroxidase (HRP) were purchased from Sigma Aldrich (St. Louis, MO, USA). *N*-acetylneuraminic acid (SA, 98%), D-galactose (99%) and L-sorbose (98%) were purchased from Aladdin Industrial Corporation (Shanghai, China). 4-Formylphenylboronic acid (FPBA, 97%), sodium cyanoborohydride (95%), D-glucose (99%) and D-arabinose (99%) were purchased from J&K Chemical (Shanghai, China). D-mannose (99%) was purchased from Alfar Aesar (Tianjin, China). 3-(4,5-Dimethylthiazol-2-yl)-2,5-diphenyltertrazolium bromide (MTT) was purchased from BDH Laboratory Supplies (Poole, Dorset, UK). Ammonium hydroxide (28% w/v) was purchased from Sinopharm Chemical Reagent (Shanghai, China). FITC-labeled *Sambucus nigra* agglutinin (SNA) was purchased from Vector Laboratories (Burlingame, CA, USA). Silver nitrate, glacial acetic acid (HAc), anhydrous methanol, anhydrous ethanol, NaH_2PO_4 and Na_2HPO_4 were purchased from Nanjing Reagent Company (Nanjing, China). Sodium dodecyl sulfate (SDS) was obtained from Bio-Rad (Hercules, CA, USA). Glass slides (18 mm × 18 mm) were from the Shanghai Glass Factory (Shanghai, China). Hepatoma carcinoma cell (HepG-2), normal hepatocyte cell (L-02), phosphate buffer solution for cell culture (1× PBS), parenzyme cell digestion solution (containing 0.25% trypase and 0.02% EDTA) and Dulbecco Modified Eagle Medium (DMEM, containing 4.5 mg/mL glucose, 80 U/mL penicillin and 0.08 mg/mL streptomycin) were purchased from Keygen Biotech (Nanjing, China). Fetal bovine serum (FBS) was purchased from Gibco (Life Technologies, Australia). The liver tissue microarray was purchased from Shanghai OutDo Biotech (Shanghai, China). All other chemical reagents were of analytical grade unless otherwise stated. Water used in all experiments was purified by a Milli-Q Advantage A10 ultrapure water purification system (Millipore, Milford, MA, USA). Glass bottom cell culture dishes (Φ 20 mm) obtained from NEST Biotechnology (Wuxi, China) were used for cell culture and

imaging.

Transmission electron microscopic (TEM) characterization was performed on a JEOL JEM-1011 TEM instrument (Tokyo, Japan). Dynamic light scattering (DLS) characterization of particle sizes was carried out on a BI-200SM (Brookhaven Instrument Corporation, Holtsville, NY, USA) instrument. UV-vis absorbance characterization was carried out on a Nanodrop-2000C instrument (Thermo Fisher Scientific, Shanghai, China). Confocal fluorescence images were recorded in the confocal laser scanning microscopy (CLSM, Zeiss LSM-710 microscope, Germany). Raman and SERS experiments were conducted on a Renishaw InVia Reflex confocal microscope (Renishaw, UK) equipped with a high-resolution grating with 1800 grooves/cm, additional band-pass filter optics, and a CCD camera. All measurements were carried out using a He-Ne laser (λ_0 = 633 nm; laser power at spot, 17 mW). For non-imaging SERS detection, the integration for Raman measurement was 3 s and SERS spectra were collected by co-addition of 5 scans. The laser was focused onto the sample by using a × 50 objective (N.A. 0.75), providing a spatial resolution of ca. 1 μm^2. Each detection was repeated 8 times at 8 different locations on the spot. Each spectrum was baseline corrected except noise test. For SERS imaging of cells, the integration for Raman measurement was 1 s and SERS spectra were collected by 1 scans. The laser was focused onto the sample by using a × 50 objective (N.A. 0.75). The step size is 1 μm. For SERS imaging of tissues, the integration and accumulation were the same as the imaging of cells. The laser was focused onto the sample by using a ×20 objective (N.A. 0.40), providing a spatial resolution of ca. 3 μm^2. The step size is 2 μm. Wavelength calibration was performed by measuring silicon wafers through a ×50 objective, evaluating the first-order phonon band of Si at 520 cm^{-1}.

Synthesis of silver NPs. Ag nanoparticles were prepared as described by Lee and Meisel.[1] In brief, $AgNO_3$ (36 mg) was dissolved in 200 mL water and brought to boil

under continuous stirring. Then, 4 mL of 1% (w/v) trisodium citrate was added. The mixture was boiled with stirring for about 1 h and then cooled down to room temperature naturally. The solution was stored at 4 °C before use.

Preparation of Ag/PATP@SiO_2 NPs. 20 μL of 1 mM PATP dissolved in ethanol was first added dropwise to 10 mL of Ag colloidal solution under rapid stirring for 40 min. To coat silica shells on the Ag/PATP NPs surfaces, a procedure described by Baida et al.[2] was employed with slight modifications. The obtained Ag colloidal solution was added with 40 mL of ethanol under stirring. Subsequently, 0.7 mL of ammonium hydroxide (28%) was added to the suspension, and the mixture was stirred for 5 min. Then 10 mL of 10 mM TEOS dissolved in ethanol was added to the suspension. The reaction was slowly stirred at room temperature for 70 min. After that, the resultant Ag/PATP@SiO_2 NPs were centrifuged at 11,000 rpm for 10 min and washed with ethanol four times followed by redispersing in 10 mL of anhydrous ethanol.

Preparation of monosaccharide-imprinted Ag/PATP@SiO_2 NPs. The molecular imprinting procedure included four steps: 1) boronic acid functionalization, 2) template immobilization, 3) oriented imprinting, and 4) template removal.

For boronic acid functionalization, amino groups were introduced by injecting 100 μL of APTMS to 10 mL of anhydrous ethanol solution containing freshly prepared Ag/PATP@SiO_2 NPs, and the mixture was stirred at room temperature for 1 h. The resulting amino-modified Ag/PATP@SiO_2 NPs were isolated by centrifugation and redispersed with 10 mL ethanol three times. The amino-modified Ag/PATP@SiO_2 NPs were dispersed in 30 mL ethanol. 300 μL of 5 mg/mL FPBA and 300 μL of 5 mg/mL sodium cyanoborohydride were added into 30 mL of Ag/PATP@SiO_2 NPs suspension. After reaction for 24 h, the solution was centrifuged and the boronic acid-functionalized Ag/PATP@SiO_2 NPs were collected via centrifuging, and then washed with ethanol and

water for three times each. Finally, the boronic acid-modified NPs were dispersed in 9 mL water.

For template immobilization, 1 ml of 3 mg/ml SA or glucose dissolved in phosphate buffer (100 mM, pH 7.4) was added into 9 mL boronic acid-modified Ag/PATP@SiO_2 NPs and the pH was adjusted to 7.4. After incubation for 30 min, monosaccharide -bound NPs were collected via centrifuging.

For oriented imprinting, the monosaccharide-bound Ag/PATP@SiO_2 NPs were redispersed into 40 mL ethanol, added with 0.7 mL ammonium water and a prepolymer solution that was consisted of 22.4 μL TEOS and 10 mL ethanol. After reaction for an appropriate duration, the reacting mixture was centrifuged and the precipitates were collected.

For template removal, the collected precipitates were washed with 0.1 M HAc for 3 h. The obtained monosaccharide-imprinted tags were collected and stored in water.

To prepare non-imprinted nanoparticles for comparison, the processing procedure was the same except that no template was immobilized onto the boronic acid-modified Ag/PATP@SiO_2 NPs.

The TEM images, dynamic light scattering (DLS) pattern, UV-vis absorption spectra and Raman spectra of the bare Ag/PATP NPs, Ag/PATP@SiO_2 NPs, SA-imprinted Ag/PATP@SiO_2 NPs and non-imprinted Ag/PATP@SiO_2 NPs are shown in Fig. S1-S4.

Boronate affinity sandwich assay. Since both the monosaccharide-imprinted and non-imprinted nanoparticles had Raman signals while the direct photometric detection of monosaccharides was difficult, the boronate affinity sandwich assay[3] was introduced to

evaluate boronic acid-modified nanotags and relevant properties of the imprinted nanoparticles, such as imprinting factor (IF), selectivity and binding dynamics. Briefly, a boronic acid-functionalized glass slide was used as a substrate, and a monosaccharide such as glucose and sialic acid was used as bridge molecule to bind with the substrate and the imprinted or non-imprinted nanoparticles. After excessive nanoparticles were removed through washing with 10 mM phosphate buffer (pH 7.4), the Raman signal of the formed glass slide-monosaccharide-nanoparticle sandwiches was detected by the Raman spectrograph.

To prepare boronic acid-modified glass slides, glass slides were first treated with 0.1 M NaOH and 0.1 M HCl for 1 h each, followed by rinse with water until neutralization (pH 7.0), and then dried in a ventilated oven at 65 °C for 30 min. Then the glass substrates were immersed in a 1:1 (v/v) mixture of APTES and methanol at 80 °C for 10 h, followed by rinse with methanol to remove residual reagents. After that, the amino-modified glass slides were immersed into a methanol solution containing 1 mg/mL FPBA and 1 mg/mL sodium cyanoborohydride at 25 °C for 10 h under continuous vibration. Finally, the glass slides were washed with methanol and water to remove residual reagents, and then dried in an oven.

To characterize the boronic acid-functionalization of glass slides, detection spots were defined by printing a cycle array with hydrophobic ink on the boronic acid-functioned slides and non-functioned slides under investigation. 10-μL samples containing HRP at 100 μg/ml and 10 μg/ml were added to the spots to incubate for 10 min. After that, each spot was rinsed with 20 μL of 0.1 M phosphate buffer, pH 8.5. Then each spot was supplemented with 10 μL TMB staining solution. After reaction for 10 min, the array was recorded with a digital camera. The results are compared in Fig. S5, which indicate successful boronic acid-functionalization of the glass slides.

Evaluation of boronic acid-functionalization of Ag/PATP@SiO_2 nanoparticles. The boronic acid-functionalization of the glass slides were immersed into glucose solution (5 mg/mL, dissolved in 0.1 M phosphate buffer, pH 7.4) for 30 min. The glass slides were washed with phosphate buffer (10 mM, pH 7.4) three times. Then, two different solutions were pipetted on glass slides and incubation for 30 min: 1) 50 μL boronic acid-functionalized Ag/PATP@SiO_2 NPs in phosphate buffer (10 mM, pH 7.4); 2) 50 μL non-functionalized Ag/PATP@SiO_2 NPs in phosphate buffer (10 mM, pH 7.4). All the glass slides were washed with phosphate buffer (10 mM, pH 7.4) three times. Finally, the Raman signal of glass slides was detected by the Raman spectrograph. The results are compared in Fig. S6, which indicate successful boronic acid-functionalization of Ag/PATP@SiO_2 nanoparticles.

Optimization of imprinting time for the preparation of SA-imprinted Ag/PATP@SiO_2 NPs. The imprinting procedure was the same as described above except that the reaction time was changed. During the reaction, an aliquot of 6 mL was taken out from the reacting mixture every five minutes (six aliquots in total), centrifuged, washed with 0.1 M HAc for 3 h, and then was centrifuged and washed by water. Finally, the monosaccharide-imprinted Ag/PATP@SiO_2 NPs were collected and dispersed in 1 mL 10 mM phosphate buffer (pH 7.4) for further evaluation. Non-imprinted Ag/PATP@SiO_2 NPs were also prepared as controls using the same processing procedure except that no template was used.

The monosaccharide-imprinted and non-imprinted Ag/PATP@SiO_2 NPs prepared above were evaluated in terms of imprinting factor through the boronate affinity sandwich assay method using SA or glucose as a bridge molecule. The above monosaccharide-imprinted and non-imprinted Ag/PATP@SiO_2 solutions prepared at each imprinting time were added with SA or glucose to get final concentration of 0.3 mg/mL and the pH was adjusted to 7.4. After incubation for 30 min, the solutions were

centrifuged and the precipitation was rinsed with 10 mM phosphate buffer (pH 7.4) three times and then dissolved in 1 mL 10 mM phosphate buffer (pH 7.4). Then, each solution was pipetted on glass slides and incubation for 30 min. After the completion of incubation, all the glass slides were washed with 10 mM phosphate buffer (pH 7.4) three times. Finally, the Raman signal of glass slides was detected by the Raman spectrograph. IF values were calculated by dividing the Raman intensity of monosaccharide-imprinted Ag/PATP@SiO_2 NPs and non-imprinted Ag/PATP@SiO_2 NPs. The results are shown in Fig. S7 and S14, which suggest that 20 min and 15 min provided the highest IF value for SA and Glc-imprinted Ag/PATP@SiO_2 NPs. Thus, 20 min and 15 min were considered as the optimal imprinting time respectively. SA and Glc-imprinted Ag/PATP@SiO_2 NPs prepared with the optimal imprinting times were used for further experiments. The dependence of the thickness of the silica layer on the polymerization time was found to be linear ($y = 0.04\ x + 0.51$, where y is in nm; x is in min),[4] thus the thickness of the imprinting layer under the optimal imprinting times was calculated to be 1.31 nm and 1.11, which is 80.9% and 84.7% of the sum of the estimated molecular lengths (1.62 and 1.31 nm, respectively) of SA and glucose (1.02 and 0.71 nm, respectively) and formylphenylboronic acid (0.6 nm) using the software ChemBioOffice 2010 (Cambridge Soft).

Absorption isotherms and binding constant measurement. A series of SA solutions with known concentrations (0.0125, 0.025, 0.05, 0.1, 0.15, 0.2, 0.25 and 0.3 mg/mL) were prepared with 10 mM phosphate buffer (pH 7.4) and their absorbance at 200 nm was measured. 15 mg SA-imprinted and non-imprinted NPs were incubated with 0.5 mL of these SA solutions, respectively. After incubation for 30 min, all the solutions were centrifuged and the absorbance of the supernatants at 200 nm was measured. The SA amounts captured by the imprinted and non-imprinted NPs, which were represented by difference between the absorbance for initial SA solutions and the corresponding supernatants, were plotted against the free concentration of the SA solutions. The

resulting absorption isotherms are shown in Fig. 2A. The K_d value of SA-imprinted NPs was estimated by the extrapolation approach as shown in Fig S8, which was estimated to be the free concentration at the horizontal axis that gave a half of the value of the maximum binding, being 2.2×10^{-4} M or 0.068 mg/mL.

Imprinting efficiency (IE). To investigate imprinting efficiency, 15 mg boronic acid-functionalized and SA-imprinted Ag/PATP@SiO_2 NPs were respectively incubated with 0.5 mL of 0.3 mg/mL SA dissolved in 10 mM phosphate buffer (pH 7.4) for 30 min. After centrifuging, the absorbance at 200 nm of the resulting supernatants was measured. IE was calculated through comparing the maximum amount of SA captured by SA-imprinted and boronic acid-functionalized Ag/PATP@SiO_2 NPs. The maximum absorbance at 200 nm for SA captured by SA-imprinted NPs from Fig. 2A was 0.0396 while the absorbance of SA captured by boronic acid-functionalized nanoparticles was 0.0920. Therefore, the IE value was 43.0%.

Binding dynamics test. 2 ml of 3 mg/ml SA in phosphate buffer (0.1 M, pH 7.4) was added into 18 mL SA-imprinted Ag/PATP@SiO_2 NPs and the pH was adjusted to 7.4. An aliquot of 3 mL was taken out of the solution at incubation time of 5, 10, 15, 20 and 30 min, centrifuged and washed with 10 mM phosphate buffer (pH 7.4) three times each. The resulting precipitation was re-dispersed in 3 mL of 10 mM phosphate buffer (pH 7.4). Then different boronic acid-functionalized glass slides rinsed with 20 μL SA-imprinted Ag/PATP@SiO_2 NPs solutions obtained at different incubation times, in 10 mM phosphate buffer, pH 7.4 and incubated for 30 min. After that, the glass slides were washed with 10 mM phosphate buffer (pH 7.4) three times. Finally, the Raman signal of glass slides was detected by the Raman spectrograph. The results are shown in Fig. S9, which suggests that a binding equilibrium was reached within 20 min.

In vitro cytotoxicity of SA-imprinted Ag/PATP@SiO_2 nanoparticles. Briefly,

HepG-2 and L-02 cells were seeded on 96-well plates with a density around 5000 cells per well and allowed to adhere for 24 h prior to the assay, respectively. The cells were co-

incubated with a series of doses of Ag/PATP@SiO_2 NPs at 37 °C for 24 h. Then, 50 μL of MTT indicator dye (5 mg/mL in PBS, pH 7.4) was added to each well, and the cells were incubated for another 4 h at 37 °C in the dark. The medium was withdrawn and 20 0 μL dimethyl sulfoxide (DMSO) was added in each well and agitated thoroughly to dis solve the formazan crystals. The solution was transferred to 96-well plates and immediately monitored on a microplate reader (Bio-Rad, Hercules, CA, USA). Absorption was measured at a wavelength of 570 nm. The cells were co-incubated with a series of doses of Ag/PATP@SiO_2 NPs at 37 °C for 24 h. Then, 50 μL of MTT indicator dye (5 mg/mL in PBS, pH 7.4) was added to each well, and the cells were incubated for another 4 h at 37 °C in the dark. The medium was withdrawn and 200 μL dimethyl sulfoxide (DMSO) was added in each well and agitated thoroughly to dissolve the formazan crystals. The values obtained were expressed as a percentage of the control cells to which no nanoparticles were added, and the cell viability was calculated by the following formula:

$$Cell\ viability(\%) = \frac{Abs(test\ cell) - Abs(backgroud)}{Abs(controlled\ cell) - Abs(backgroud)} \times 100\%$$

The measured cytotoxicity of Ag/PATP@SiO_2 NPs toward HepG-2 and L-02 cells at different Ag/PATP@SiO_2 NPs doses are shown in Fig. S10.

Stability and repeatability of the SERS intensity of the SA-imprinted Ag/PATP@SiO_2 NPs. We investigated the stability of the SERS intensity of SA-imprinted SERS nanotags in three aspects: 1) The SERS intensity of the same batch of material under the same experimental conditions at different times within a same day (run-to-run repeatability); 2) the SERS intensity of the same batch material under the same experimental conditions at different days (day-to-day repeatability); 3) The SERS intensity of the different batches of material under the same experimental conditions

(batch-to-batch repeatability). 10 μL of SA-imprinted Ag/PATP@SiO_2 NPs was dropped onto a glass substrate and allowed to dry naturally. For all the measurements, each detection was repeated 8 times at 8 different locations on the spot, the integration for Raman measurement was 1 s and SERS spectra were collected by 1 scans. The results are showed in Fig. S11.

Selectivity test. Boronic acid-functionalized glass slides were used for the experiments. Each glass slide was pipette on equivalent volumes of 10 mM phosphate buffer (pH 7.4) with 5 mg/mL glucose, mannose, galactose, sorbose, arabinose and SA, respectively and incubated for 30 minutes. After incubation, the glass slides were washed with 10 mM phosphate buffer (pH 7.4) three times and then were rinsed with 20 μL SA or Glc-imprinted Ag/PATP@SiO_2 NPs solution in 10 mM phosphate buffer, pH 7.4 and incubated for 30 min. After that, the glass slides were washed with 10 mM phosphate buffer (pH 7.4) three times. Finally, the Raman signal of glass slides was detected by the Raman spectrograph. The results for SA-imprinted Ag/PATP@SiO_2 NPs are shown in Fig. 2B while those for Glc-imprinted Ag/PATP@SiO_2 NPs are showed in Fig. S15.

We investigated the stability and repeatability of the selectivity of SA-imprinted SERS nanotags in two aspects: 1) The selectivity of SA-imprinted SERS nanotags of the same batch at different times; 2) The selectivity of SA-imprinted SERS nanotags of the different batches at the same experimental condition. We investigated the selectivity of SA-imprinted nanotags that have prepared for one month and the results are shown in Fig. S13. We investigated the selectivity of SA-imprinted nanotags of other two batches and the results are shown in Fig. S14.

Cell culture and SERS imaging. HepG-2 and L-02 were cultured in DMEM medium with 10% fetal bovine serum for 2 to 3 days (37 °C, 5% CO_2). The cell culture medium was removed and the cells remained on the cell culture dishes were washed with 1×

PBS for two times. Then the cells were respectively incubated with 1 ml boronic acid-functionalized, SA-imprinted, Glc-imprinted and non-imprinted Ag/PATP@SiO_2 NPs (300 μg/mL each) dissolved in 1× PBS for 20 min. The PBS buffer and free nanoparticles were removed and the remaining cells were rinsed with 1× PBS for three times. Then the cells were fixed with 3.7% paraformaldehyde for 20 min, and washed twice with PBS and supplemented with 1 mL 1× PBS. The obtained cells were directly observed under the Raman microscope. To investigate the influence of the presence of monosacchrides on cell imaging, the cells were respectively incubated with SA-imprinted NPs which were preblocked with SA and glucose (200 μg/mL each) dissolved in 1× PBS for 20 min. The PBS buffer and nanoparticles were removed and the remaining cells were rinsed with 1× PBS for three times. Then the cells were fixed with 3.7% paraformaldehyde for 20 min, and washed twice with PBS and supplemented with 1 mL 1× PBS. The obtained cells were directly observed under the Raman microscope.
We investigated the stability and repeatability of cell imaging by SA-imprinted SERS nanotags in two aspects: 1) Cell imaging via the SA-imprinted SERS nanotags of the same batch at different times; 2) Cell imaging via SA-imprinted SERS nanotags of additional two batches under identical experimental conditions. We first examined the selectivity of cell imaging by SA-imprinted SERS nanotags that has prepared for one month. The results are showed in Fig. S19. We further investigated prepared the selectivity of cell imaging by SA-imprinted SERS nanotags of other two batches. The results are showed in Fig. S20.

Cell imaging by the FITC-labeled SNA. Briefly, 300 μL of the HepG-2 and L-02 cells were seeded, at 4 × 106 cells/mL, on glass coverslips and incubated at 37 °C for 24 h with 5% CO_2 respectively. Following this period of incubation, 30 μL of the FITC-labeled SNA was added to each coverslip and again incubated for 1 h at 37°C with 5% CO_2. The coverslips were then washed in triplicate with a 1× PBS to fixing the cells to the coverslips using 4%-paraformaldehyde at 37 °C for 2 min. Following this period,

the coverslips were again washed with 1× PBS followed by washing with sterile water before allowing it to air-dry for 2 h. The coverslips were then mounted to glass slides using DPX mountant prior to analysis. Fluorescence images of SNA-FITC-tagged HepG-2 and L-02 cells are shown in Fig. S18.

Tissue Imaging. Tissue sections were put in a ventilated oven at 63 °C for 1 h to melt the paraffin. Then tissue sections were incubated in xylene to remove paraffin (15 min ×2) and then immersed in a degraded ethanol series (100%, 95%, 80%, 70%, water and PBS) each for 5 min to rehydrate. After washing with PBS buffer, the hydrated tissue sections were heated in citrate buffer (0.01 M, pH 6.0) at 37 °C for 3 min to retrieve antigens. Then the spots of the cancer and normal liver tissues were respectively incubated with 10 μL of 300 μg/mL SA-imprinted and non-imprinted Ag/PATP@SiO_2 NPs dissolved in 1× PBS for 20 min. The PBS buffer and free NPs were removed and the remaining cells were rinsed with 1× PBS for three times. The obtained cells were directly observed under the Raman microscope.

References：

1) P. C. Lee and D. Meisel, *J. Phys. Chem.-Us*, 1982, **86**, 3391-3395.
2) H. Baida, P. Billaud, S. Marhaba, D. Christofilos, E. Cottancin, A. Crut, J. Lerme, P. Maioli, M. Pellarin, M. Broyer, N. Del Fatti, F. Vallee, A. Sanchez-Iglesias, I. Pastoriza-Santos and L. M. Liz-Marzan, *Nano Lett.*, 2009, **9**, 3463-3469.
3) J. Ye, Y. Chen and Z. Liu, *Angew. Chem. Int. Ed.*, 2014, **53**, 10386-10389.
4) Z.J. Bie, Y. Chen, J. Ye, S.S. Wang and Z. Liu, *Angew. Chem. Int. Ed.*, 2015, **54**, 10211-10215.

Supplementary data

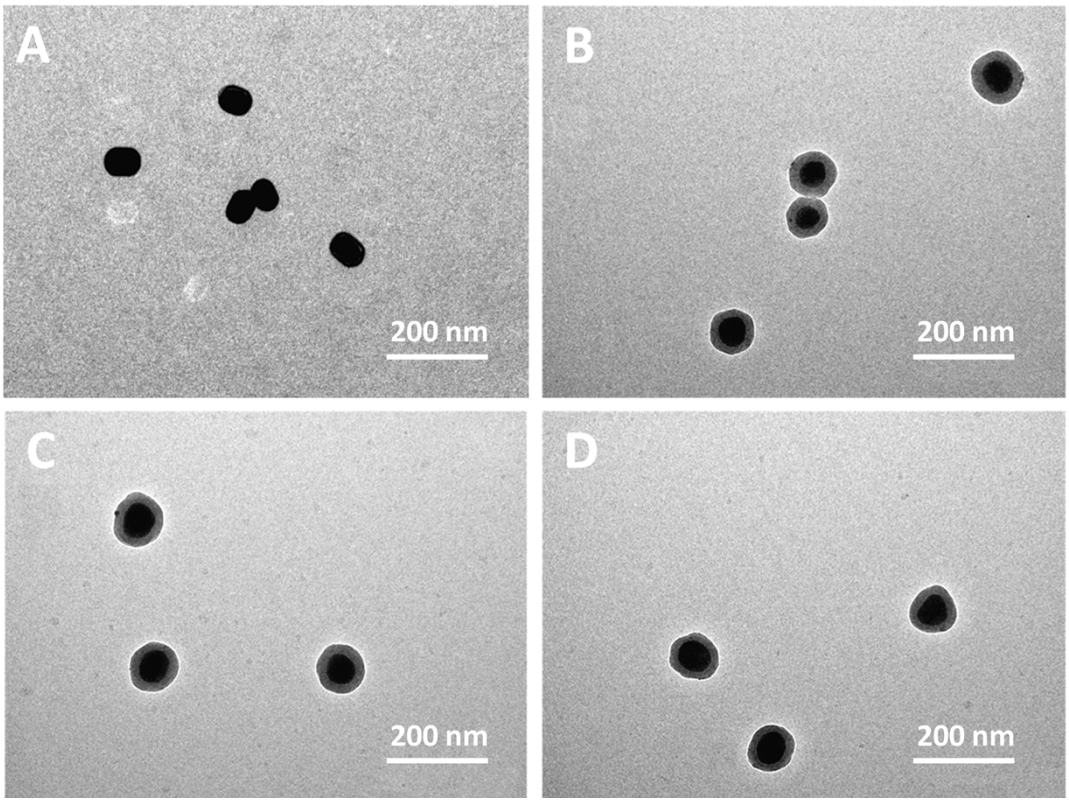

Fig. S1. TEM characterization of Ag/PATP NPs (A), Ag/PATP@SiO_2 NPs (B), SA-imprinted Ag/PATP@SiO_2 NPs (C) and non-imprinted Ag/PATP@SiO_2 NPs (D).

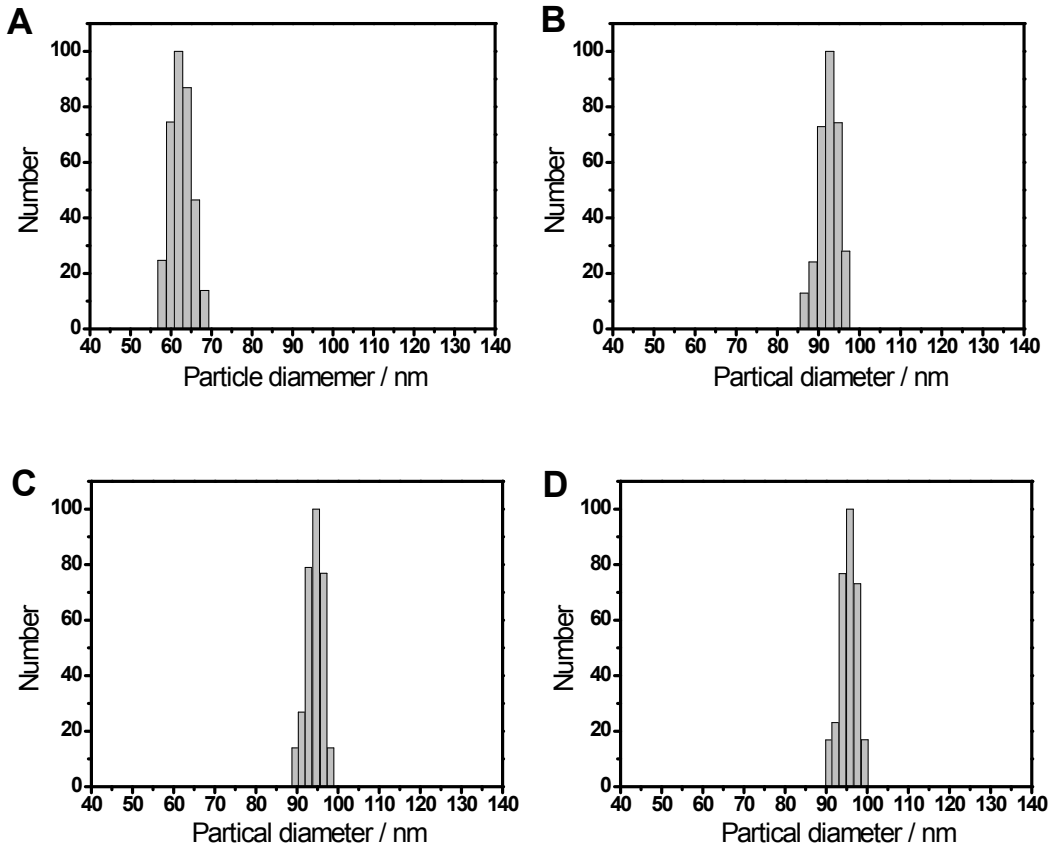

Fig. S2. DLS characterization of Ag/PATP NPs (A), Ag/PATP@SiO_2 NPs (B), SA-imprinted Ag/PATP@SiO_2 NPs (C) and non-imprinted Ag/PATP@SiO_2 NPs (D).

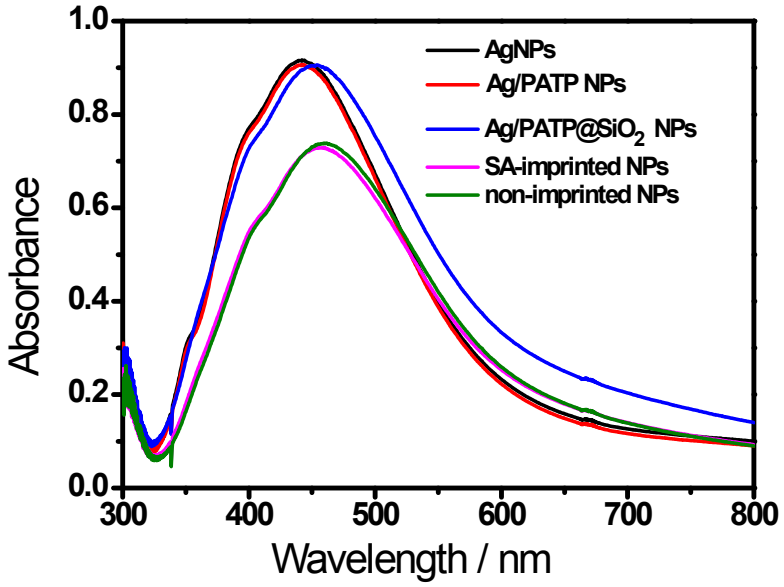

Fig. S3. UV-vis absorption spectra of bare AgNPs, Ag/PATP NPs, Ag/PATP@SiO_2 NPs, SA-imprinted Ag/PATP@SiO_2 NPs and non-imprinted Ag/PATP@SiO_2 NPs.

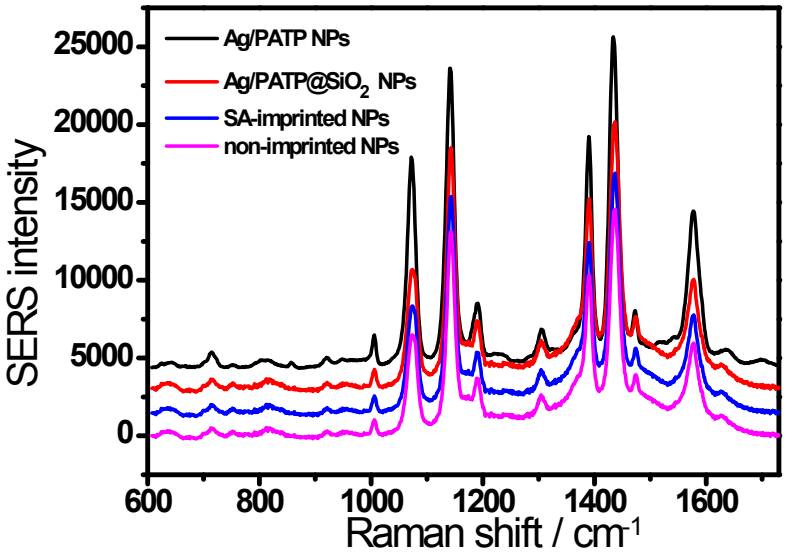

Fig. S4. SERS spectra of Ag/PATP NPs, Ag/PATP@SiO_2 NPs, SA-imprinted Ag/PATP@SiO_2 NPs and non-imprinted Ag/PATP@SiO_2 NPs.

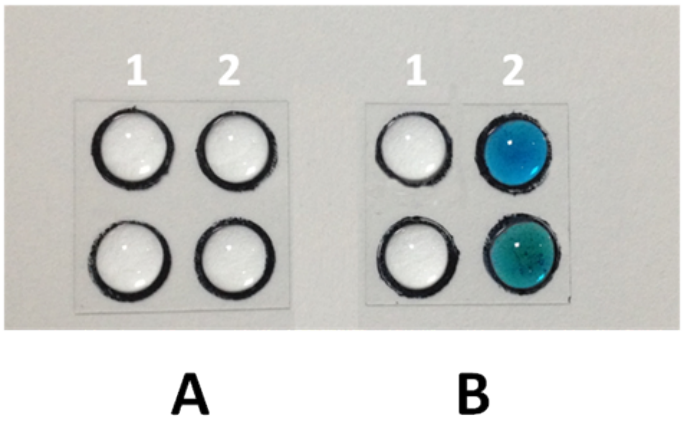

Fig. S5. Photo images for boronate affinity sandwich assay on non-functionalized glass slide (A) and boronic acid-functionalized glass slide (B). Sample: A1 and B1, 0.1 M phosphate buffer, pH 8.5; A2 and B2, 10 μg/ml HRP dissolved in 0.1 M phosphate buffer, pH 8.5.

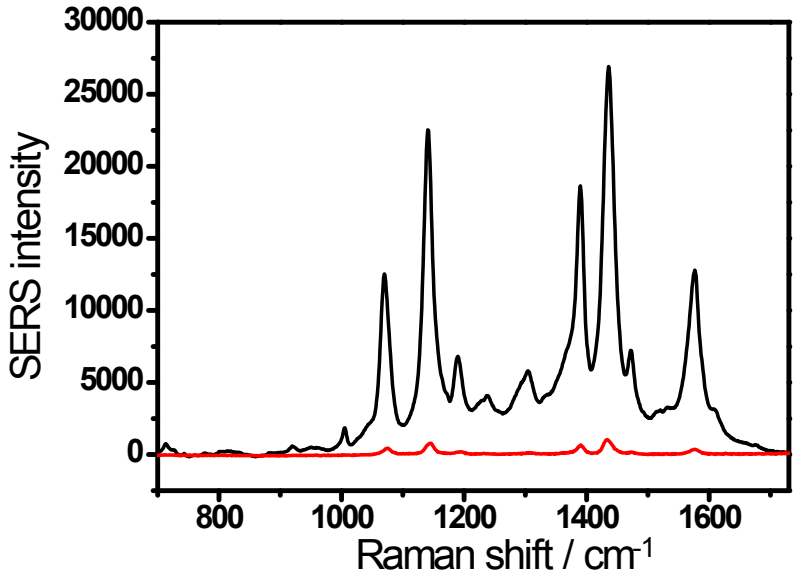

Fig. S6. Raman intensity of boronic acid-functionalized Ag/PATP@ SiO_2 NPs (black) and non-functionalized Ag/PATP@SiO_2 NPs (red) detected through the boronate affinity sandwich assay.

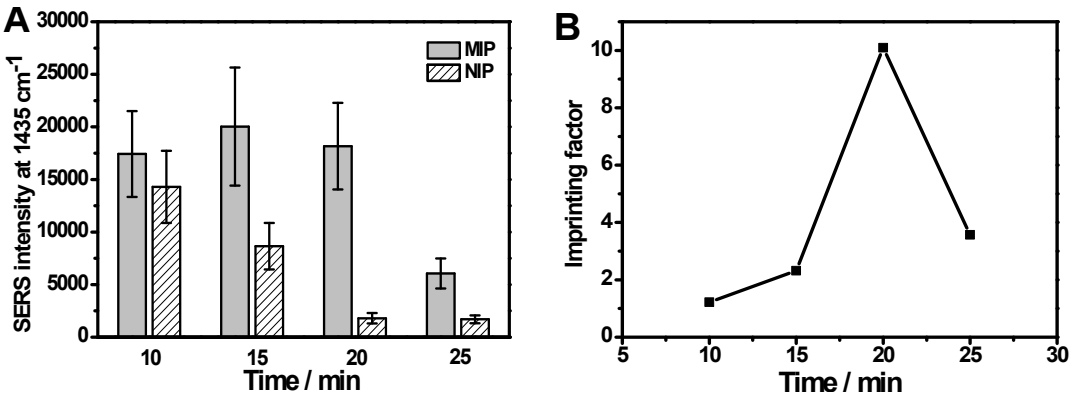

Fig. S7. SERS intensity of SA-imprinted and non-imprinted NPs prepared at different imprinting time (A) and dependence of imprinting factor on imprinting time (B).

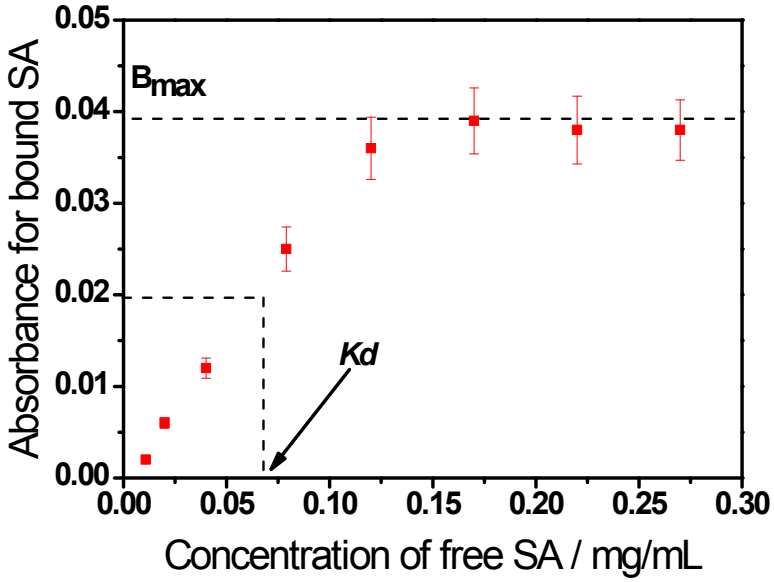

Fig. S8. Binding isotherms for binding of the SA-imprinted NPs to SA.

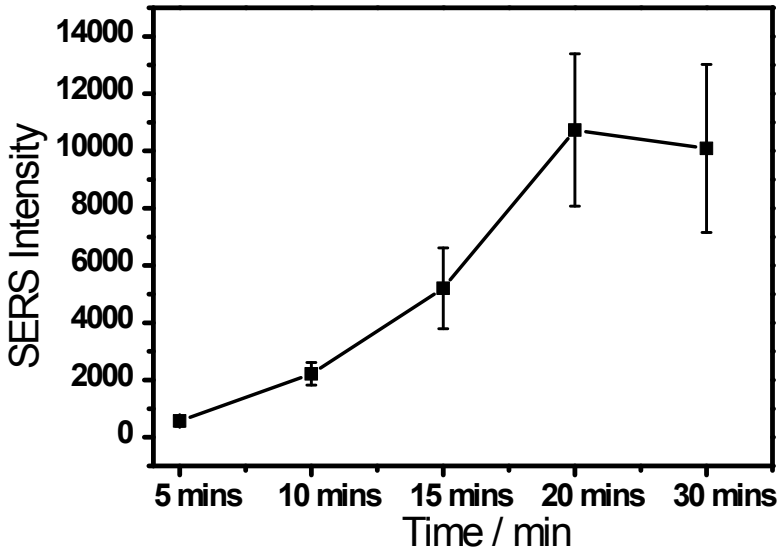

Fig. S9. Dependence of the SERS intensity for SA captured by SA-imprinted NPs on the incubation time with SA.

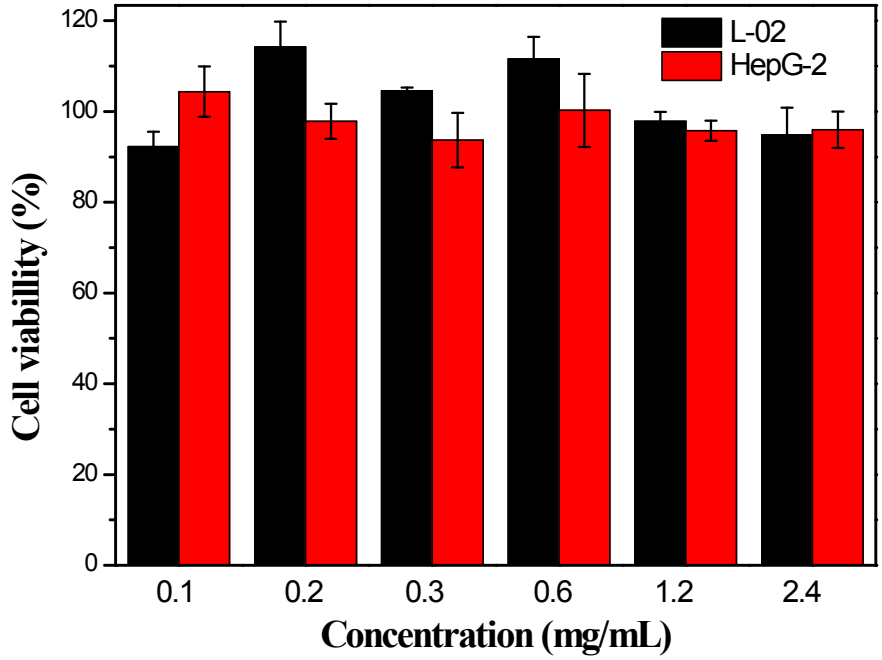

Fig. S10. In vitro cytotoxicity of SA-imprinted Ag/PATP@SiO_2 NPs toward HepG-2 and L-02 cells at different concentration of SA-imprinted Ag/PATP@SiO_2 NPs.

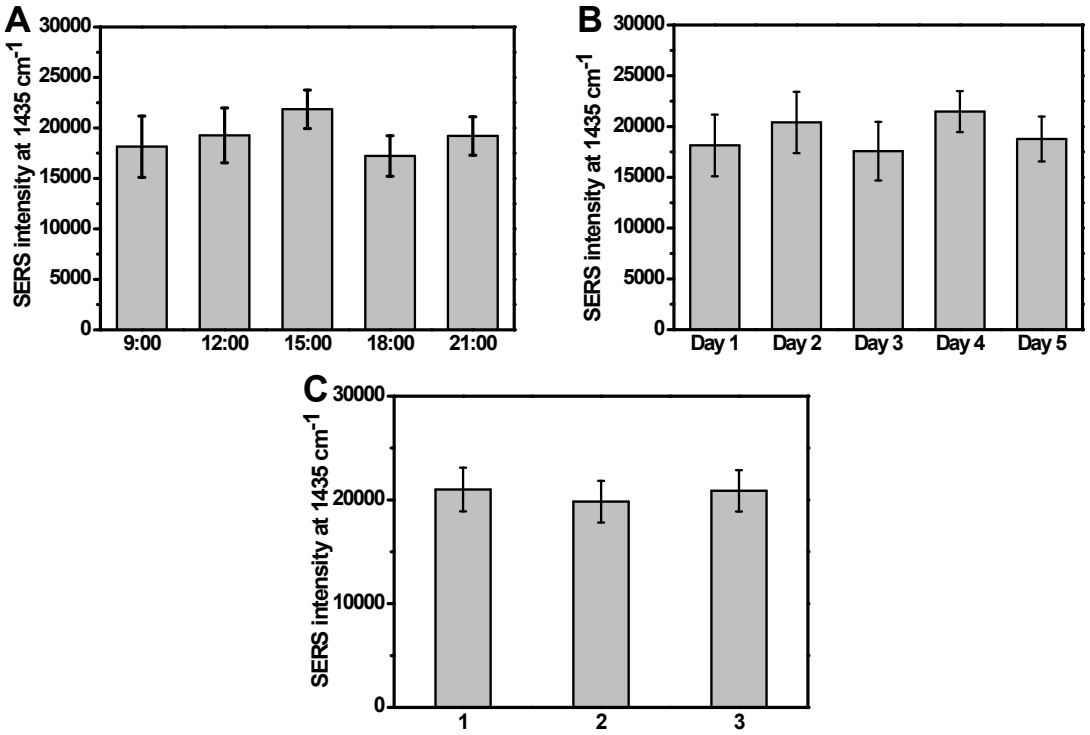

Fig. S11. The SERS intensity of the same batch of SA-imprinted NPs detected at different time within the same day (A), different days (B) and three batches of SA-imprinted NPs detected at different times (C) under identical experimental conditions.

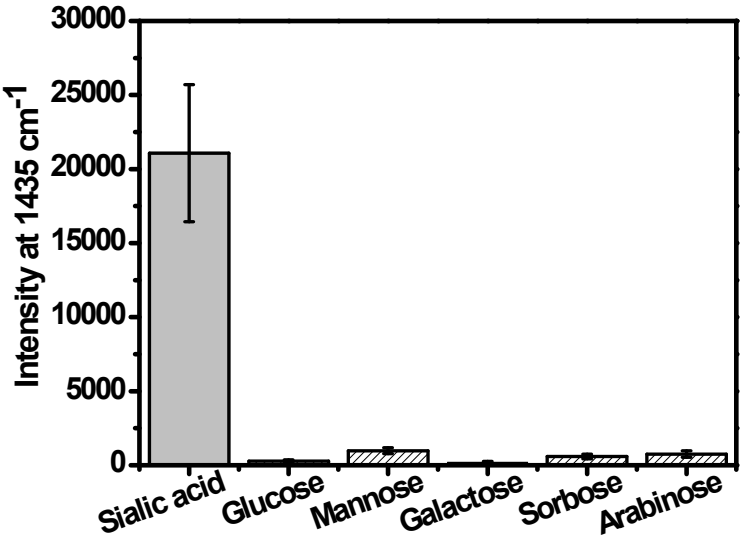

Fig. S12. The selectivity of SA-imprinted NPs after stored for one month toward different monosaccharides.

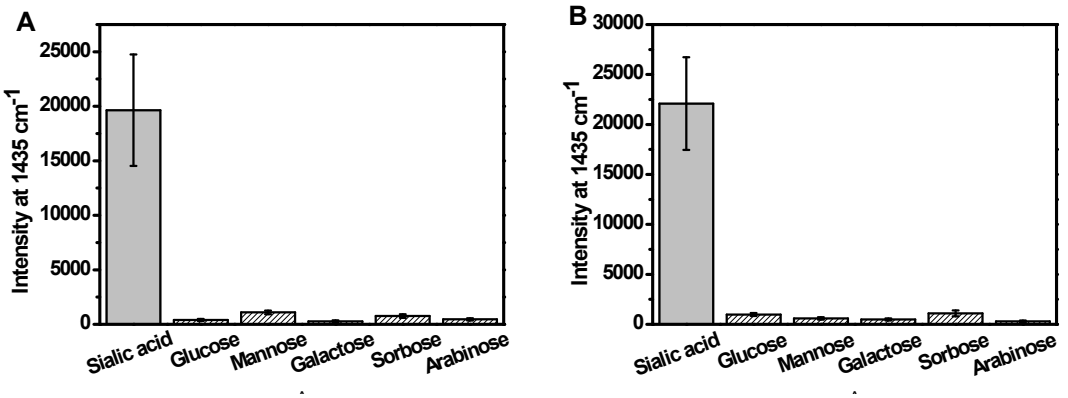

Fig. S13. The selectivity of another two batches of the SA-imprinted NPs toward different monosaccharides.

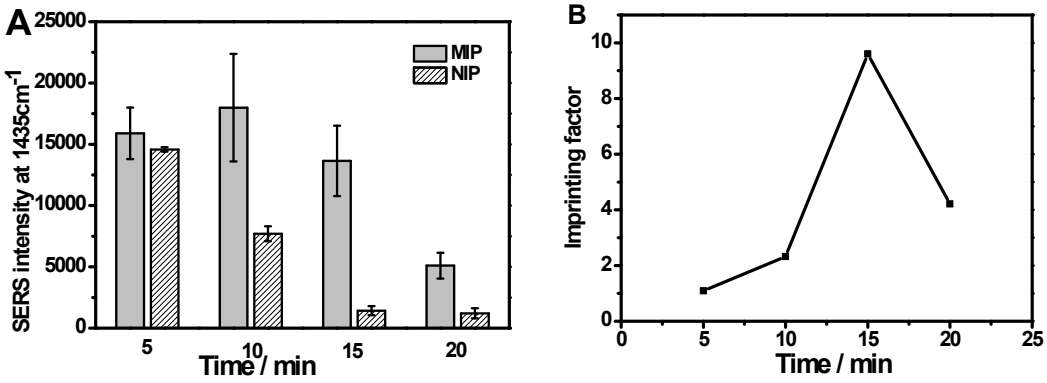

Fig. S14. SERS intensity of Glc-imprinted and non-imprinted NPs prepared at different imprinting time (A) and dependence of imprinting factor on imprinting time (B).

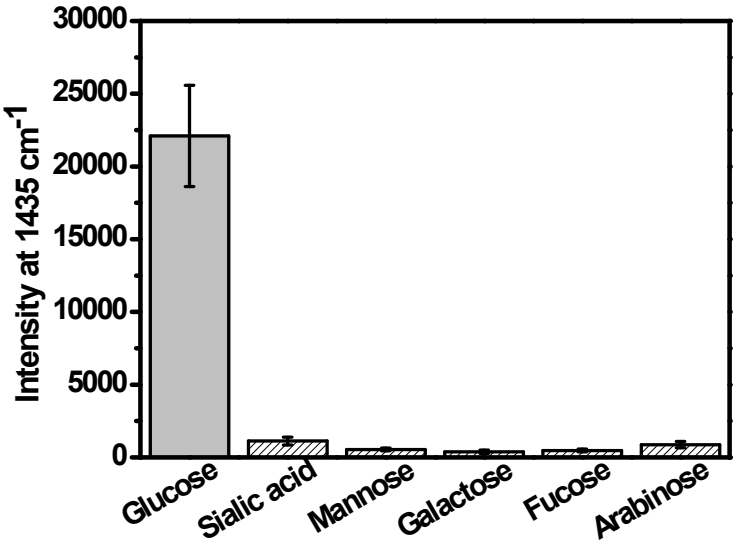

Fig. S15. The selectivity of Glc-imprinted NPs toward different monosaccharides.

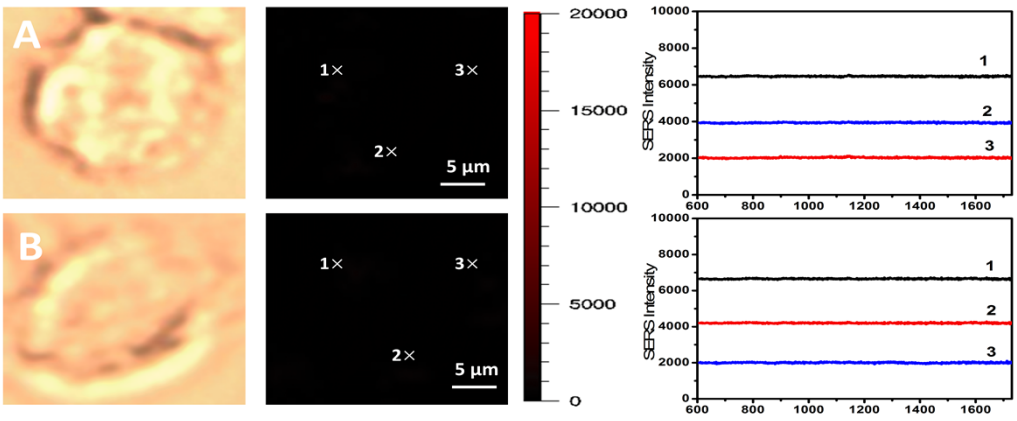

Fig. S16. SERS imaging of HepG-2 (A) and L-02 cells (B) after incubated with Glc-imprinted SERS nanotags. Columns from left to right: bright field, SERS image and representative SERS spectra taken at three locations on cell surfaces as indicated in the dark-field images.

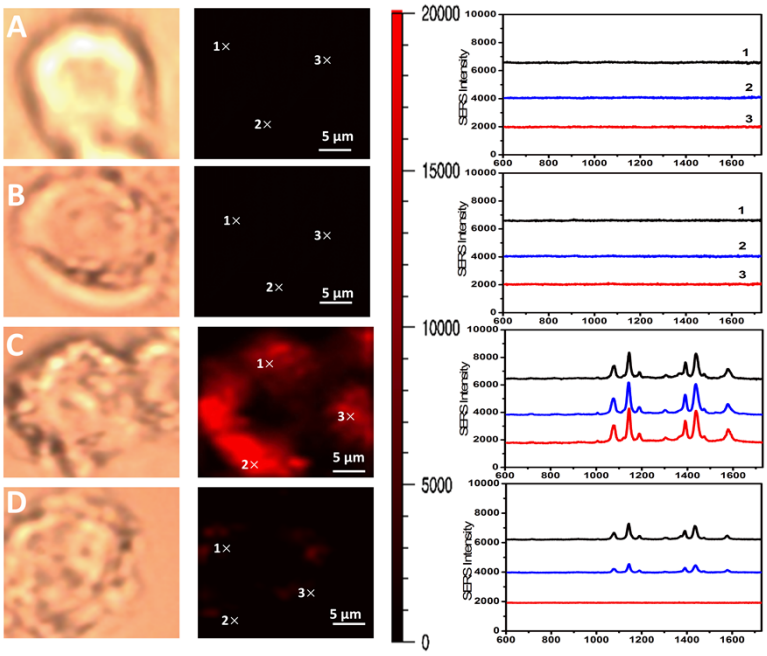

Fig. S17. Confocal SERS imaging of HepG-2 cell (A, C) and L-02 (B, D) cell after incubated with SA-imprinted NPs in the presence of different monosaccharides (300 μg/mL). A and B: sialic acid; C and D: Glucose.

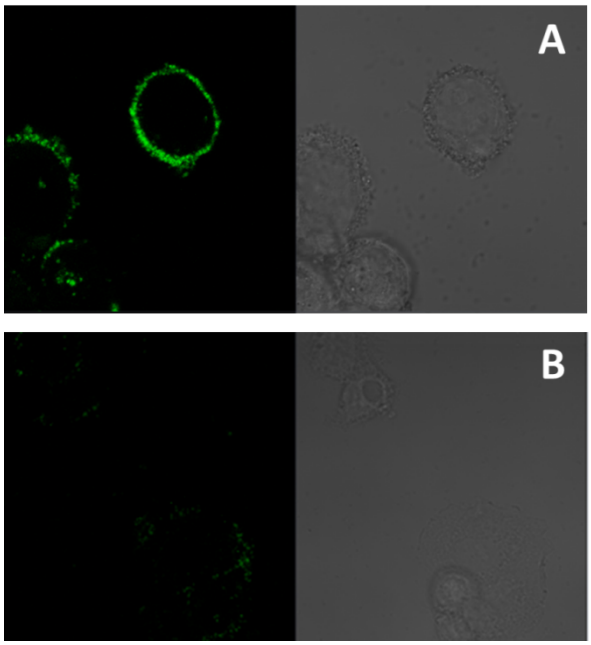

Fig. S18. Fluorescence images of HepG-2 (A) and L-02 cells (B) after incubated with FITC-labeled SNA. Columns from left to right: Bright field cell images, fluorescence images of FITC-labeled SNA tagged cells.

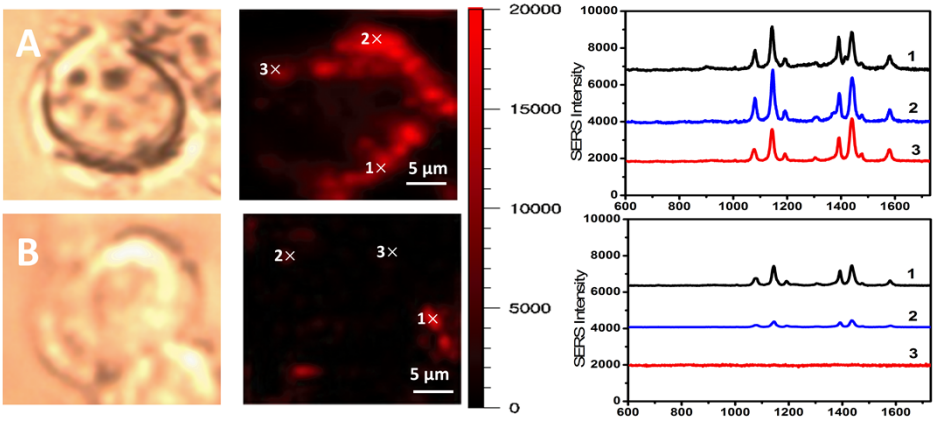

Fig. S19. Confocal SERS imaging of HepG-2 cells (A) and L-02 cells (B) after incubated with SA-imprinted NPs prepared one month ago. Columns from left to right: bright field, SERS image and representative SERS spectra taken at three locations on cell surfaces as indicated in the dark-field images.

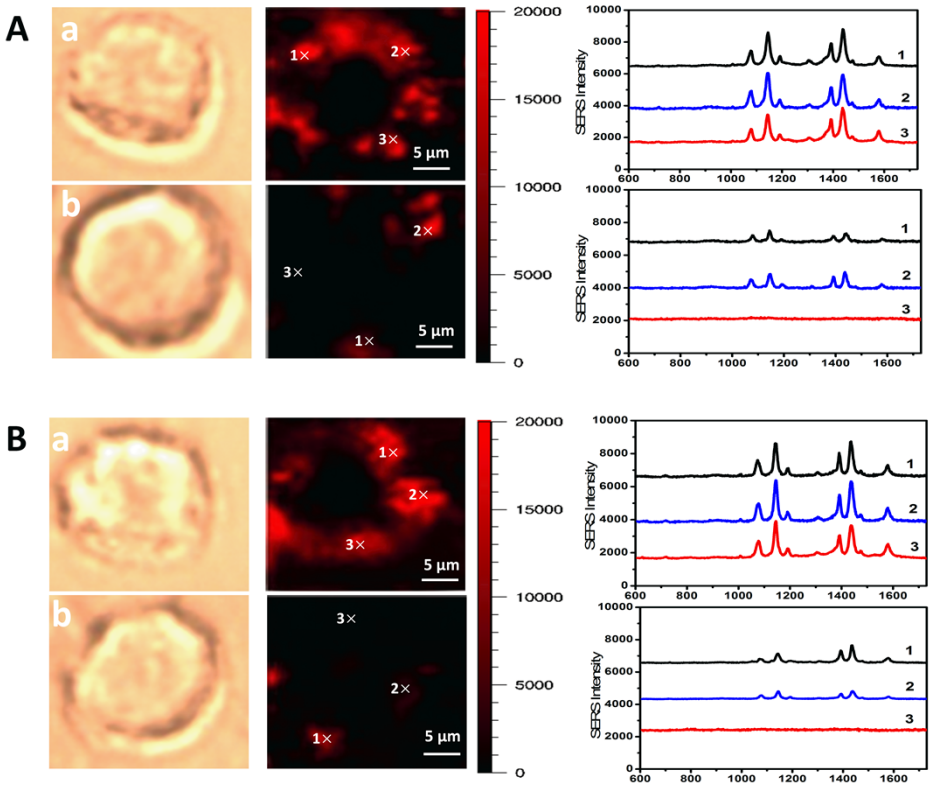

Fig. S20. SERS imaging of cancer and normal cells after incubated with SA-imprinted NPs of a second and third batch (A, B). a) HepG-2 and b) L-02 cells after incubation with the SA-imprinted NPs. Columns from left to right: bright field, SERS image and representative SERS spectra taken at three locations on cell surfaces as indicated in the dark-field images. Results for the first batch are shown in Fig. 3.